Molecular and Cellular Biochemistry **286:** 161–170, 2006.
DOI: 10.1007/s11010-005-9108-0

Identification and characterization of recombinant and native rat myristoyl-CoA: protein N-myristoyltransferases

Vincent Rioux,[1] Erwan Beauchamp,[1] Frédérique Pedrono,[1] Stéphanie Daval,[1] Daniel Molle,[2] Daniel Catheline[1] and Philippe Legrand[1]

[1]*Laboratoire de Biochimie, INRA-Agrocampus, 35042 Rennes, France;* [2]*UMR STLO, INRA-Agrocampus, 35042 Rennes, France*

Received 9 November 2005; accepted 8 December 2005

Abstract

Compared to other species that possess a single functional myristoyl-CoA: protein N-myristoyltransferase gene copy, human, mouse and cow possess 2 NMT genes, and more than 2 protein isoforms. In mammals, the contribution of each gene transcript to multiple protein isoform expression and enzyme activity remains unclear. In order to get new insight on their respective physiological role, we have cloned and characterized the two rat NMT cDNAs. Rat NMT1 and NMT2 cDNAs contain 1491 and 1590 nucleotides, respectively, with high identity with their mouse homologues. Polypeptide sequences exhibited 68.1% identity between NMT1 and 2. Recombinant rat NMT1 and 2 showed major immunoreactive forms at 66 and 50 kDa, although NMT2 is 33-amino acid longer than NMT1. Both proteins exhibited functional myristoyltransferase activity but NMT2 appeared to be 4-time less active than NMT1. Studies of native protein expression revealed that the level and sizes of NMT proteins greatly vary among rat tissues although NMT1 and 2 did not display tissue specific expression at the mRNA level. Altogether, these results suggest that NMT2 may contribute little to total NMT activity levels in vivo. (Mol Cell Biochem **286:** 161–170, 2006)

Key words: NMT, N-terminal myristoylation, myristic acid, saturated fatty acid metabolism, rat

Abbreviation: NMT, myristoyl-CoA: protein N-myristoyltransferase; hNMT, human NMT

Introduction

Protein N-myristoylation refers to the covalent attachment of myristic acid (C14:0), by an amide linkage, to the NH_2-terminal glycine residue of increasing number of eukaryotic and viral proteins [1]. The proteins that are substrates of myristoyltransferase (NMT) include key components in intracellular signaling pathways [2], oncogenes [3], structural viral proteins [4] and common constitutive eukaryotic proteins [5]. Computational prediction recently suggested that about 0.5% of all proteins in the human genome could be myristoylated [6] and that the Arabidopsis thaliana myristoylome could represent 1.7% of the complete proteome [7]. The functional significance of the myristoyl moiety has been shown to mediate protein subcellular localization, protein-protein interaction or protein-membrane interactions required for the biological activities of the myristoylated proteins [1]. Therefore, in the myristoylation pathway, the fatty acid substrate myristic acid exhibits a specific and important role

Address for offprints: P. Legrand Laboratoire de Biochimie INRA-Agrocampus 65 rue de Saint-Brieuc, CS 84215 35042 RENNES Cedex, FRANCE (E-mail: Philippe.Legrand@agrocampus-rennes.fr)

for protein activation and, consequently, for cell regulation.

Myristoyl-CoA: protein N-myristoyltransferase (NMT, EC 2.3.1.97), the enzyme catalyzing this stable acylation, has been identified in yeast [8, 9], insects [10], plants [7, 11, 12], unicellular parasites [13, 14] and some mammals [15–17]. Although this enzyme has been well characterized in fungi, since the three-dimensional structure of *C. albicans* NMT [18], as well as the structure of the *S. cerevisiae* NMT ternary complex [19] have been determined, there are still unresolved questions concerning the mammalian NMTs. Genetic advances have revealed that at least 3 mammalian species (human, mouse and bovine) possess 2 distinct NMT genes, named type 1 and 2 [17, 20]. The specific role of each NMT isoform in cellular processes, especially the contribution of each gene transcript to NMT expression and activity in vivo, remains unclear. A comparison of the activity of recombinant human NMT1 and NMT2 has suggested that they have similar substrate selectivity [17]. Recent results showing that NMT1-deficient mice are not viables [21] have shown that the 2 enzymes are however not functionally redundant in normal tissues during embryogenesis, since NMT1-deficiency was not rescued by the presence of NMT2 in early mouse development. In the mouse, therefore, NMT1 but not NMT2 is considered as an essential gene involved in early embryonic development [21]. Finally, another study [22] that especially focused on cancer cells showed that both human NMT1 and NMT2 possess myristoylation activity, but only NMT1 is involved in the control of cellular replication and tumor cell proliferation.

To date, rat NMT genes have not been described, but biochemical studies have shown that rat tissues possess a myristoyltransferase activity [15, 23]. By using ^{3}H-myristic acid metabolic labeling followed by 2D electrophoresis, we have also demonstrated the presence of myristoylated proteins in cultured rat hepatocytes [24, 25]. The aim of the present work was to identify and characterize the two rat NMT cDNAs and to study their respective expression and activity in a recombinant cellular model. These information were further used to analyze the expression of native rat NMT1 and NMT2 in vivo. These results will contribute to more fully understand the regulatory mechanisms involved in myristoylated protein synthesis and to elucidate the physiological role of rat NMT1 and NMT2, as compared to what is known with the mouse and human genes.

Materials and methods

Chemicals

Radiolabeled [1-^{14}C]-myristic acid was purchased from Sigma (St-Quentin Fallavier, France). Fetal calf serum (FCS) was obtained from Perbio (Bezons, France). Reagents for electrophoretical application were purchased from Amersham BioSciences (Orsay, France) and BioRad (Marnes-la-Coquette, France). Solvents (HPLC grade) came from Fisher Scientific (Elancourt, France). Other chemicals were obtained from VWR (Fontenay-sous-Bois, France) or from Sigma.

5′- and 3′-Rapid Amplification of cDNA Ends

Mouse NMT1 and NMT2 cDNA [17] (GenBank Accession Numbers NM_008707 and NM_008708, respectively) were used to Blast-search the rat genomic database. Rattus Norvegicus chromosome 10 supercontig NW_047340 presented high identity with mouse NMT1 and chromosome 17 supercontig NW_047496 presented high identity with mouse NMT2. Based on these genomic sequences, a set of oligonucleotide primers specific for each rat cDNA was designed (Table 1) to obtain their 5′- and 3′-ends. The 5′- and 3′-RACE reactions were performed with rat liver Marathon-Ready cDNA library (Clontech, Ozyme, France) using the high fidelity *Pfu* polymerase (Promega, Lyon, France). The PCR products were sequenced using the dideoxy-nucleotide-chain-termination method, either directly or after cloning into the pGEM-T-easy vector system (Promega).

Plasmid constructions

Plasmids coding for rat NMT1 and NMT2 were constructed for expression in mammalian cells. Oligonucleotide primers were designed (Table 1) to PCR amplify the full-length rat NMT1 and NMT2 coding sequences from the rat liver Marathon-Ready cDNA library. The cloning NMT1 forward primer included the translation start codon and *Hind*III restriction site. The cloning NMT1 reverse primer contained the translation stop codon and *Xho*I restriction site.

Due to the high sequence homology of rat NMT1 and NMT2, a nested PCR was designed to obtain rat NMT2 cDNA. The 1st round of PCR was made with oligonucleotides designed in the 5′ and 3′ UTR and a 2nd round of PCR was subsequently made with a NMT2 forward primer that included the translation start codon and *BamH*I restriction site and a NMT2 reverse primer that contained the translation stop codon and *Xba*I restriction site.

The resulting 1491-bp and 1590-bp PCR products were cloned into the pcDNA3 (Invitrogen, Cergy Pontoise, France) expression vector (*Hind*III and *Xho*I sites for NMT1 and *BamH*I and *Xba*I sites for NMT2). In-frame orientations were confirmed by DNA sequencing. These plasmids are referred as pcDNA3/NMT1 and pcDNA3/NMT2. The sequences of full-length rat NMT1 and NMT2 cDNAs are available in

Table 1. Primers designed for rapid amplification of cDNA ends, cloning and quantitative RT-PCR analyses of rat NMT genes

Primer name	Sequence	position[a]
For 5′- and 3′-RACE		
rNMT1-5RACE1	5′-CCTCCTCGTTCTCGCAATCG-3′	93–112
rNMT1-5RACE2	5′-GATCCTCTCTGCTGGCAAAGAG -3′	246–267
rNMT1-5RACE3	5′-GGCCGGAGAGCCCACAAGAG -3′	589–608
rNMT1-3RACE	5′-GCTCAAGTTCGGCATAGGGG-3′	1392–1411
rNMT2-5RACE	5′-CAGATGCGGAGTCGGACTTG -3′	192–211
rNMT2-3RACE	5′-GGGAGACGAAGAAGTG-3′	1197–1212
AP1	5′-CCATCCTAATACGACTCACTATAGGGC-3′	–
AP2	5′-ACTCACTATAGGGCTCGAGCGGC-3′	–
For cloning		
rNMT1-CLONF[b]	5′-CAAAAGCTT*ATG*GCGGATGAGAGTGAGACAGC-3′	1–23
rNMT1-CLONR	5′-CGTGCTCGAG*CTTA*CTGTAACACCAACCCAACCT-3′	1469–1491
rNMT2-CLON1F	5′-CTCGGAGCCGCCGCG*ATG*-3′	(−)15–3
rNMT2-CLON2F	5′-CAAGGATCCGAATTC*ATG*GCGGAGGACAGCGAG-3′	1–18
rNMT2-CLON1R	5′-CAGCCTTCTAGGAATAACATCC-3′	1593–1614
rNMT2-CLON2R	5′-CAATCTAGACTCGAG*CTA*CTGTAGAACAAGTCC-3′	1573–1590
For qPCR		
RNMT-qPCRF	5′-TGTACCGGCTGCCAGAGACT-3′	977–996
rNMT1-qPCRR	5′-AGCTGGTGCACTACCGGAAT-3′	1036–1055
rNMT1-qPCRprobe	5′-FAM-CAAGACAGCTGGGCTACGCCCGAT-3′-TAMRA	999–1022
rNMT2-qPCRF	5′-AGAGCAGTCCGAGAGCTAATCAA-3′	1138–1160
rNMT2-qPCRR	5′-GAACCAGTGGGCCACTTCTTC-3′	1204–1224
rNMT2-qPCRprobe	5′-FAM-TACTTGAAGCAGTTTCATCTAGCTCCA-3′-TAMRA	1165–1191

[a]Primer positions represent nucleotide positions on rat NMT1 and NMT2 cDNAs starting at the first ATG codon, as described in accession numbers NM_148891 and NM_207590.
[b]In italics are the start or stop codon, underlined are the restriction sites used for cloning.

the GenBank database (accession numbers NM_148891 and NM_207590, respectively).

Cell culture and transfection

Rat NMT1 and NMT2 were expressed by transiently transforming COS-7 cells with pcDNA3/NMT1 and pcDNA3/NMT2. COS-7 cells were routinely maintained at about 50% confluence and cultured in Dulbecco′s modified Eagle′s medium (DMEM) containing 10% FCS, 50 IU/mL penicillin and 50 μg/mL streptomycin. The cells were split 1 day before transfection to 50% confluence, and transfected the following day using the EasyJect Plus electroporator (Equibio, Monchelsea, UK) according to the manufacturer's instruction. Briefly, 10^6 cells in 0.8 mL DMEM were mixed with 30 μg of purified plasmid, electroporated at 250 V and 1,500 μF with unlimited resistance, and seeded on a 10 cm dish (Falcon, AES, Combourg, France) containing culture medium. In order to normalize for transfection efficiency, 3 μg of a plasmid coding for β-galactosidase (pcDNA3.1/*lacZ*) was co-transfected with each assay.

NMT activity assay

The assay for NMT activity was adapted from that described first by Towler and Glaser [26]. COS-7 cells were washed twice with PBS and scraped into PBS. After centrifugation, the cell pellet was resuspended in 50 mmol/L phosphate buffer (pH 7.4) containing 0.25 mol/L sucrose and sonicated at 20 W for 10 s [27]. The protein content of the cell homogenate was determined by a modified Lowry procedure [28]. NMT activity was assayed in a 100 μL mixture containing 5 μL of cell homogenate (25-50 μg protein), 150 mM phosphate buffer (pH 7.2), 6 mM $MgCl_2$, 7 mM ATP, 0.5 mM CoA and 100 μM of peptide substrate. The peptide substrate (GAQLSTLSRV) used in this work (from Sigma Genosys, Haverhill, UK) has a sequence similar to the 10 amino-terminal residues of rat NADH-cytochrome b5 reductase, a well-known substrate of NMT [29]. The reaction was started by adding 10 nmol of [1-^{14}C]-myristic acid (20 mCi/mmol) and stopped with 100 μL methanol and 10 μL TCA (100% w/v) after 15 min of incubation at 37 °C. Proteins were precipitated for 10 min at 0 °C and centrifuged (10,000 g, 10 min, 4 °C). The supernatant (100 μL) was analyzed

by HPLC (Alliance integrated system, Waters, St Quentin en Yvelines, France) using a Nova-Pak C18 column. The separation was performed by elution (1 mL/min) with a linear gradient of water (0.1% TFA):acetonitrile (0.1% TFA) starting at 70:30 (v/v) and increasing to 0:100 (v/v) in 35 min. Peaks corresponding to radiolabeled myristoylpeptide and myristic acid were collected and subjected to liquid scintillation counting. From the amount of radioactivity found in the substrate and product, the enzyme activities could be determined and expressed as pmol myristoylpeptide produced per min per μg of protein. Myristoyltransferase activities were normalized for transfection efficiency by measuring the β-galactosidase activity [30]. Unambiguous identification of the myristoylpeptide was made by nano Liquid Chromatography/Mass Spectrometry (LC/MS) showing the free peptide ($m/z = 1031.58$) and the myristoylpeptide ($m/z = 1241.77$) which is coherent with a 210 Da mass increase corresponding to the amide linkage to the myristoyl group (data not shown).

Rat tissue preparation

Tissues from Sprague-Dawley male rats were rapidly dissected, weighed and homogenized in 4 volumes (w/v) of sucrose 0.25 M, KH_2PO_4 10 mM, Na_2HPO_4 40 mM (pH 7.4) containing 200 mM PMSF, aprotinin 200 mM and leupeptin 10 mM. The homogenates were centrifuged at 10,000 g (30 min, 4 °C). The resulting supernatant was centrifuged at 100,000 g, 1 h, 4 °C in order to separate the cytosolic from the microsomal fraction.

RNA isolation and real-time quantitative PCR

Real-time quantitative PCR was used to determine the relative abundance of NMT1 or NMT2 in rat tissues. Total RNA was isolated from 100 mg-tissue samples using Trizol reagent (Invitrogen). Two μg of total RNA was reverse transcribed with random hexamers using SuperScript II reverse transcriptase (Invitrogen). PCR mixture contained 2 μL of the resulting cDNA (diluted 5 times), 500 nM of forward and reverse primers, 250 nM of dual labeled (5′-FAM, 3′-TAMRA) fluorogenic probe (Eurogentec) and PCR Master Mix (Applied Biosystems) in a total volume of 40 μL. The mRNA abundance relative to 18S rRNA was measured using the Comparative C_T (Threshold Cycle) Method according to the manufacturer's instructions.

Western blotting

Reduced protein samples were analysed by SDS-PAGE and blotted onto nitrocellulose (Amersham Biosciences, Les Ulis, France). Membranes were probed with affinity-purified anti-human NMT1 (hNMT1) rabbit polyclonal antibodies generously provided by Dr. Cravatt (The Scripps Research Institute) [17]. Rabbit antibodies were revealed with horseradish-peroxidase-conjugated sheep anti-rabbit IgG (Sigma). Peroxidase activity was revealed by following the procedure provided for the ECL Plus system kit (Amersham Biosciences).

Results

Isolation and cloning of the rat NMT cDNAs

Alignment of the mouse NMT1 and NMT2 cDNAs to the rat genomic database enabled us to localize fragments of sequences encoding rat NMT1 on chromosome 10 (NW_047340) and fragments of sequences encoding rat NMT2 on chromosome 17 (NW_047496). Interestingly, a region of chromosome 5 (NW_047716) also presented a high similarity with mouse NMT1 cDNA, but did not contain the putative start codon localized at the most upstream 5′-end nor any exon-intron structure. Specific primers were subsequently designed (Table 1) to identify the 5′- and 3′-flanking regions of these sequences by RACE reactions with a rat liver cDNA library used as a template.

Concerning NMT1, a single 5′-extension PCR fragment of 180 bp was obtained using rNMT1-5RACE1 oligonucleotide (Table 1) designed in the 1st potential exon. Sequence analysis of this rat NMT1 5′ region identified a candidate ATG translation site, 12 bp upstream of this 1st site, and the adaptator primer 2 sequence. In the 3′-end, two PCR products of 300 and 400 bp were obtained by using rNMT1-3RACE oligonucleotide. As shown after sequencing, only the lower band corresponded to the 3′-end of rat NMT1, revealing the stop site and 203 bp downstream this site. Computational analyses of the obtained 5′ and 3′ NMT1 sequences showed that they share total identity with the rat genomic database (NW_047340). Tentative 5′-extension using rNMT1-5RACE2 and rNMT1-5RACE3 (Table 1) designed in the 3rd and 5th exon failed to demonstrate any other potential alternative splice variant at the 5′ end in the rat liver cDNA library (data not shown).

Concerning NMT2, 5′- and 3′-extensions using rNMT2-5RACE and rNMT2-3RACE oligonucleotides (Table 1), respectively, resulted in a confirmation of the genomic sequences (NW_047496) available in the database: 15 bp upstream of the start codon and 32 bp downstream of the stop codon.

Based on these results, full-length rat NMT1 (accession #NM_148891) and NMT2 (accession #NM_207590) cDNAs were amplified by PCR using specific primers (Table 1) and cloned into the pcDNA3 plasmid. Rat full-length NMT1

```
RatNMT2 MAEDSESA----ASQLSLELDD----QDTCGIDGDNEEETEHAKG--SPGRDLGAKKKKK    50
RatNMT1 MADESETAVKLPAPSLPLMMEGNGNGHEHCS-DCENEEDISHNRGGLSPANDTGAKKKKK    59

RatNMT2 KQKRKKEKPNSGGTKSDSASDSQEIKIQQSSKHNAIWQQISAGAAMGGDTMEGEWIDLRM    110
RatNMT1 KQKKKKEK----GNDMDSTQD-QPVKMN------------------------------    81

RatNMT2 YHKNPTIPIQKLQDIQRAMELLSACQGPARNIDEATKRRYQFWDTQPVPKLNEVITSHGA    170
RatNMT1 -----SLPAERIQEIQKAIELFSVGQGPAKTMEEASKRSYQFWDTQPVPKLGEVVNTHGP    137

RatNMT2 IEPDKDNIRQEPYSLPQGFMWDTLDLSNAEVLKELYTLLNENYVEDDDNMFRFDYSPEFL    230
RatNMT1 VEPDKDNIRQEPYTLPQGFTWDALDLGDRGVLKELYTLLNENYVEDDDNMFRFDYSPEFL    197

RatNMT2 LWALRPPGWLLQWHCGVRVSSNKKLEGFISAIPANIRIYDSVKRMVEINFLCVHKKLRSK    290
RatNMT1 LWALRPPGWLPQWHCGVRVVSSRKLVGFISAIPANIHIYDTEKKMVEINFLCVHKKLRSK    257

RatNMT2 RVAPVLIREITRRVNLEGIFQAVYTAGVVLPKPVATCRYWHRSLNPRKLVEVKFSHLSRN    350
RatNMT1 RVAPVLIREITRRVHLEGIFQAVYTAGVVLPKPVGTCRYWHRSLNPRKLIEVKFSHLSRN    317

RatNMT2 MTLQRTMKLYRLPDVTKTSGLRPMEPKDIRAVRELINVYLKQFHLAPVMGDEEVAHWFLP    410
RatNMT1 MTMQRTMKLYRLPETPKTAGLRPMEKKDIPVVHQLLSRYLKQFNLTPVMNQEEVEHWFYP    377

RatNMT2 REHIIDTFVVESPSGKLTDFLSFYTLPSTVMHHPAHKSLKAAYSFYNIHTETPLLDLMND    470
RatNMT1 QENIIDTFVVENANGEVTDFLSFYTLPSTIMNHPTHKSLKAAYSFYNVHTQTPLLDLMSD    437

RatNMT2 ALIIAKLKGFDVFNALDLMENKTFLEKLKFGIGDGNLQYYLYNWRCPGTDSEKVGLVLQ     529
RatNMT1 ALVLAKMKGFDVFNALDLMENKTFLEKLKFGIGDGNLQYYLYNWKCPSMGAEKVGLVLQ     496
```

Fig. 1. Comparison of the deduced amino acid sequences of rat NMT1 (NM_148891) and NMT2 (NM_207590). Amino acids that are conserved between sequences are shaded.

(1491 bp) and NMT2 (1590 bp) both share 95% identity with their published respective mouse cDNA homologues and 90 and 88%, respectively, with their human homologues [17]. A comparison between rat NMT1 and NMT2 cDNAs revealed a sequence identity of 68.5%. Alignment of the deduced polypeptide sequences exhibited 68.1% identity between rat NMT1 and NMT2 (Fig. 1).

Further alignment of the obtained cDNAs to the rat genomic sequences by computational analyses showed that rat NMT1 gene contains 12 exons and spans about 33 kb on chromosome 10, with a gap between exons 9 and 10. As already mentioned above, chromosome 5 supercontig NW_047716 nucleotides 147349 to 145992 shares 86% identity with rat NMT1 (starting nt61 to nt1491) with no exon/intron structure. Rat NMT2 gene contains 14 exons. Surprisingly, 21 bp of the rat NMT2 cDNA localized between nt 90 and 110 after the ATG start are lacking on the rat genomic database. This fragment is present on the mouse and human NMT2 cDNAs.

Expression of rat NMT1 and NMT2 in COS-7 cells

Western blot analyses were performed on samples from COS-7 cells expressing rat NMT1 or NMT2 (Fig. 2), by using the affinity-purified anti-hNMT antibodies raised against a fragment (residues 89-496) of human NMT1 that is conserved in human NMT2 [17]. Control cells (lane 1) showed a weak immunoreactive band at 66 kDa that probably corresponds to COS-7 cell NMT basal expression. Rat NMT1 (lane 2) led to 6 immunoreactive bands with apparent molecular weights of 66, 65, 60, 52, 50 and 45 kDa. Rat NMT2 (lane 3), although theoretically 33 amino acid longer than NMT1, yielded 2 major bands with apparent molecular weights of 66 and 50 kDa and a weak band at 45 kDa. Fig. 2 shows that both recombinant rat cDNA products were revealed by the antibodies. Since each sample was loaded after β-galactosidase activity normalization, Fig. 2 suggests that anti-NMT antibody has less affinity for rat NMT2 than for rat NMT1.

Functional activity of recombinant rat NMT1 and NMT2

As shown Fig. 3, both recombinant enzymes exhibited functional myristoyltransferase activity, i.e. were able to catalyze in vitro the formation of a myristoylated peptide from a decapeptide substrate similar to the N-terminus of rat NADH-cytochrome b5 reductase (GAQLSTLSRV) and from myristic acid. Recombinant NMT1 and NMT2 activities were linear up to 60 min of incubation time (Fig. 3A). Myristoyltransferase activity increased linearly (Fig. 3B) with each recombinant protein amount (cell homogenate volume). Both activities showed a saturation with myristic acid (Fig. 3C) and peptide substrate (Fig. 3D) concentrations higher than 100 μM. In these experimental conditions, compared to NMT1 and after β-galactosidase normalization, recombinant NMT2

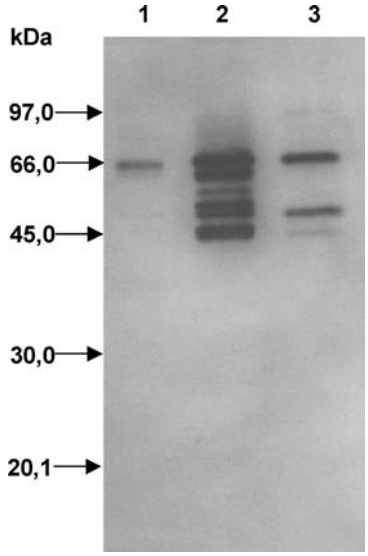

Fig. 2. Immunoblot of recombinant rat NMT proteins expressed in COS-7 cells. Lane 1: control (not transfected) COS-7 cells; lane 2: COS-7 cells transfected with pcDNA3/NMT1; lane 3: COS-7 cells transfected with pcDNA3/NMT2. COS-7 cell homogenates (10 μg protein per lane with normalization to β-galactosidase activity) were resolved by SDS-PAGE and blotted. The membrane was probed with polyclonal anti-NMT antibodies directed against a conserved fragment of human NMT1 and NMT2 [17].

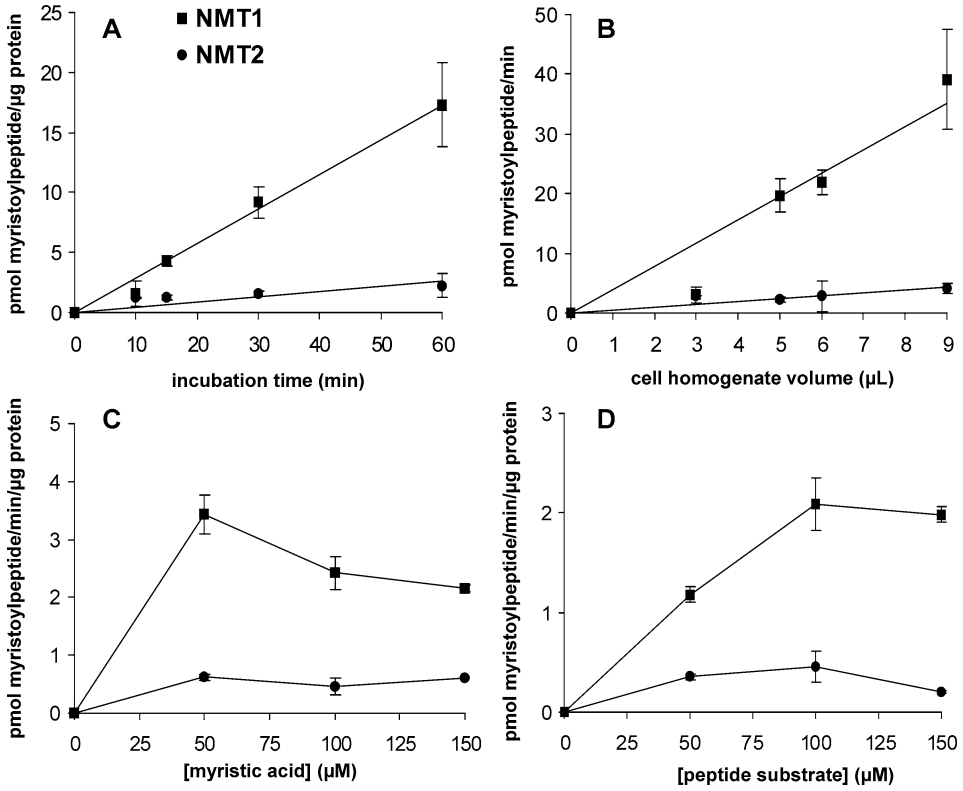

Fig. 3. N-myristoyltransferase activities of COS-7 cells expressing rat NMT1 or NMT2. Results are expressed as a function of incubation time (A), incubated cell homogenate volume (B), myristic acid (C14:0) concentration (C) and peptide substrate concentration (D). Myristoyltransferase activity was calculated from the amount of radiolabeled myristoylated peptide produced, normalized for transfection efficiency by measuring the β-galactosidase activity. Values are means $\pm$ SD, $n = 3$.

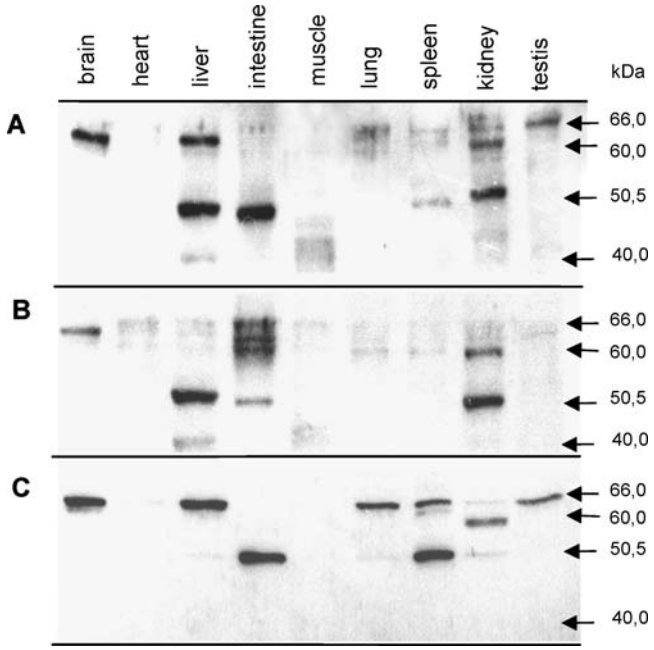

Fig. 4. Distribution of NMT proteins in rat tissues and subcellular fractions. Samples (20 μg protein) from post-mitochondrial supernatant (A), cytosolic (B) and microsomal (C) fractions from rat tissues were separated by SDS-PAGE and transferred onto a nitrocellulose membrane. The membrane was probed with polyclonal anti-NMT antibody directed against a conserved fragment of human NMT1 and NMT2 [17]. This figure shows the results obtained with 1 rat but is representative of 3 different tissue preparations from 3 rats.

appeared to be consistently 4-time less active than NMT1 (Fig. 3).

Tissue distribution of rat NMT proteins

Using the anti-NMT antibody that was demonstrated above to detect both rat NMT gene products, we examined the distribution of NMT proteins in various rat tissues. Depending on the tissue and the subcellular fraction analyzed (Fig. 4), the antibody yielded 1 to 4 bands with apparent molecular weights of approximately 66, 60, 50 and 40 kDa. The higher band (66 kDa) was present in almost every tissues and seemed to be predominantly microsomal (Fig. 4C). The band at 60,000 was shown specifically in the kidney (Fig. 4A, 4B and 4C). In the liver, 3 bands were shown, the middle one (50 kDa) being the more expressed (Fig. 4A). In the heart, skeletal muscle and lung, almost no expression of NMT was evidenced. These results show that, although the antibody cannot discriminate between NMT1 and NMT2, rat possess distinct NMT protein profiles depending on the tissue analysed.

Tissue distribution of rat NMT1 and 2 mRNA

In order to discriminate between the 1 and 2 genes, the level of NMT1 and NMT2 mRNA was measured by real-time quantitative PCR in the rat tissues analysed above for protein expression. The accuracy of the method was first verified on RNA samples from COS-7 cells expressing either rat NMT1 or NMT2 (data not shown) demonstrating that each pair of primers designed for real-time PCR (Table 1) is really specific for only one NMT cDNA. Our results are expressed as NMT1 (Fig. 5A) or NMT2 (Fig. 5B) mRNA tissue level relative to rat liver. Fig. 5 shows that, as opposed to results obtained at the protein level, both NMTs are expressed by most rat tissues and that the 2 genes share the same tissue pattern of mRNA level. There is therefore no evidence for a relationship between the protein profiles and the mRNA profiles. Finally, to test the hypothesis that the differences in NMT protein sizes may derived from alternative splicing at the 5′-end of the NMT1 gene rather than from protein processing, a PCR screening of rat tissue cDNAs by rNMT1-CLONF/rNMT1-5RACE2 (Table 1) was undertaken, showing that whatever the tissue analyzed, a single expected PCR product of about 280 bp was found (data not shown).

Discussion

The aim of the present work was to identify and characterize the rat NMT genes and to study their respective expression and activity in a recombinant cellular model. These

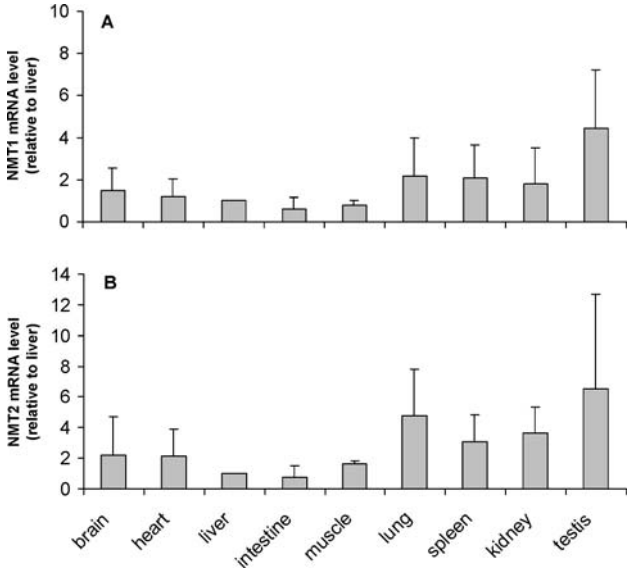

Fig. 5. Distribution of NMT1 (A) and NMT2 (B) mRNA in rat tissues. mRNA levels were determined by real-time quantitative RT-PCR analyses as described in Materials and Methods. The tissue mRNA abundance relative to 18S rRNA was calculated using the Comparative C_T (Threshold Cycle) Method and expressed using liver as a reference. Values are means ± SD, $n = 3$.

information were further used to analyze the expression of native rat NMT1 and NMT2 in vivo. Indeed, in mammals, the contribution of each gene transcript to multiple protein isoform expression and enzyme activity remains unclear.

Firstly, our results show that rat possess 2 distinct NMT cDNAs on chromosomes 10 and 17 that correspond to the type 1 and 2 NMTs (Fig. 1) already described in mouse and human [17]. Full-length rat NMT1 and NMT2 open-reading frames contain 1491 and 1590 nucleotides, respectively, and share high identity (95%) with their published respective mouse cDNA homologues [17]. Fungi, insects, and plants have been shown to possess a single NMT gene copy, except *Arabidopsis Thaliana* where the 2nd cDNA does not seem to have usual myristoyltransferase activity [7]. Mammalian species (human, mouse, cow, and now rat) possess therefore specifically 2 NMT genes [17, 20].

The 1st original cDNA encoding a mammalian NMT was isolated by Duronio et al. [31] more than 10 years ago. This human open-reading-frame of 1248 nucleotides encoded a 416 amino-acid polypeptide (Mr=48,109) that was functionally active when expressed in *E. Coli*. Since then, the cDNA encoding this human NMT1 has lengthened by 5′-extension to reach 1491 nucleotides [16, 17, 32], like the full-length rat NMT1 cDNA isolated in our work (Fig. 1). However, a controversy still exists on the real length of the human cDNA at the 5′-end and on the genomic organization of human NMT1 on chromosome 17 [33]. In our study, sequence analysis of the rat NMT1 5′ region identified a candidate ATG translation site and 12 bp upstream of this 1st site, suggesting that the transcriptional start point of full-length rat NMT1 is localized upstream of this ATG site. In addition, our result strongly suggest that there is no evidence for an alternative splice variant of rat NMT1 mRNA 110 bp shorter than the longest one (data not shown), as described in the human sequence [16]. Human and mouse NMT2 have been isolated more recently [17], followed by bovine NMT2 [20], suggesting a higher level of genetic complexity in mammals than in other species.

Recombinant rat NMT1 transiently transfected in COS-7 cells by the single plasmid pcDNA3/NMT1 led to 6 distinct proteins forms, with apparent molecular weights of 66, 65, 60, 52, 50 and 45 kDa (Fig. 2) none of which corresponding to the predicted molecular mass of 56.9 kDa. The 5′-end of full-length rat NMT1 cDNA is characterized by the presence of 5 potential in-frame ATG start codon at nucleotide positions 1, 55, 58, 211 and 241. When expressed as an N-terminal 3X-Flag fusion protein, rat NMT1 led to a unique band at 68 kDa (data not shown) which suggests that the 66-kDa form (Fig. 2) is the full-length one. Recombinant human NMT1 also showed several isoforms with aberrant migration on SDS-PAGE [17]. In addition, this study also showed weakly immunoreactive 67- and 64-kDa proteins that were present in mock-transfected cells [17]. In our study, a single band at 66 kDa was evidenced in control cells. In both studies, these bands probably corresponds to COS-7 cell NMT endogenous basal expression, although low specificity of the antibody cannot be excluded. On the human NMT1 sequence, 4 successive potential translation start sites have been proposed

[16, 17, 31, 32] and the N-terminal extension of human NMT1 containing polylysine residues (amino acid residues 55 to 67 in the rat sequence, Fig. 1) has been suggested to be involved in targeting the protein to the ribosomes but was not required for recombinant activity [32].

The fact that recombinant rat NMT2 led to 3 bands (Fig. 2), with molecular weights (66, 50 and 45 kDa) totally similar to rat NMT1, increases the complexity of this study. Full-length rat NMT2 is theoretically 33 amino acid longer than NMT1, with a predicted molecular mass of 60.6 kDa. Compared to NMT1, it is more difficult to explain the existence of these forms by the presence of additional ATG start codon on the rat sequence, since they are localized at nucleotide positions 1, 286, 301, 328. A previous study on human NMT2 expression [17] showed that hNMT2 appeared as a single 65-kDa protein, corresponding to the highest one shown in the rat. Altogether, the similarity in the molecular weights obtained with NMT1 and NMT2 is in favour of post-translational protein processing for both recombinant proteins together with the presence of multiple start codons in the rat NMT1 sequence. In addition, artifactual proteolysis or low specificity of the antibody initially raised against human NMT1, not rat NMT1 and NMT2, cannot be excluded.

COS-7 cells expressing either rat NMT1 or NMT2 showed significantly higher levels of myristoyltransferase activity in vitro than control cells (Fig. 3). The peptide substrate used in this work has a sequence similar to the N-terminus of rat NADH-cytochrome b5 reductase (GAQLSTLSRV). This protein has been shown to be myristoylated in vivo [5] and in vitro [29]. An important result of this study is that although both recombinant proteins exhibited functional myristoyltransferase activity, NMT2 appeared to be consistently 4-time less active than NMT1 (Fig. 3). Concerning previous results obtained with human NMT1 and NMT2, Giang and Cravatt [17] did not found significant differences in human NMT activity, but they transfected 4-time less hNMT1 plasmid than hNMT2 plasmid to obtain comparable expression level, which is finally coherent with our results. When transposed in vivo, these results may indicate that NMT2 contributes little to total NMT activity level in normal tissues, as also suggested by the great reduction of NMT activity in NMT1 −/− embryonic stem cells [21].

All the data obtained in the recombinant model can now be used to analyze the complexity of rat tissue-specific NMT mRNA and protein expression. Native rat NMT protein expression reproducibly showed major immunoreactive bands at 66, 60, 50 kDa and a minor band at 40 kDa, depending on the tissue analysed (Fig. 4). Identical molecular weights, except the lowest form at 40 kDa have been shown in the recombinant model expressing NMT1 (Fig. 2). Two of them (66 and 50 kDa) are also characteristic of recombinant NMT2 expression (Fig. 2). The finding of a protein form at 66 kDa in a great number of rat tissues argues in favor of the functionality of the 1st ATG start in rat NMT1 sequence. Since the antibody cannot discriminate between NMT1 and NMT2, it is not possible to state positively the contribution of each gene transcript to the 66 and 50-kDa isoform expression. However, this suggests that the form at 60 kDa may come from NMT1 rather than NMT2 gene. As opposed to multiple protein expression in normal tissues, a recent study on native NMT1 and NMT2 in cancer cell lines evidenced a single protein isoform for each gene product with a similar molecular weight of about 60 kDa [22]. It is likely that NMT protein synthesis is disturbed in cancer cells compared to normal tissues, since NMT has been described as a potential chemotherapeutic target for cancer [22, 34].

The analysis of the subcellular localization of the isoforms suggests that the higher band (66 kDa) is predominantly microsomal (Fig. 4), whereas the 60 and 50-kDa middle-forms are found in both the cytosolic and microsomal fractions. The lower band at 40 kDa was shown only in the cytosolic fraction. The results obtained in the recombinant model suggest that the native 66-kDa form corresponds to full-length rat NMT1 or NMT2, therefore containing the polylysine residues thought to be involved in targeting the protein to the ribosomes [32].

Although the western blot analyses were not done quantitatively, apparent contradiction appeared between the tissue NMT protein levels (Fig. 4) and mRNA levels (Fig. 5). Indeed, Fig. 5 shows that NMT1 and NMT2 mRNA are expressed by most rat tissues and that the 2 genes share the same pattern of mRNA level. Northern blot analyses of human and mouse tissues also showed that both NMT are widely expressed [17]. More recently, northern blot analyses suggested a regular higher tissue level of NMT1 than NMT2 mRNA in adult mice [21]. In this study [21], NMT1 mRNA expression was high in early embryogenesis and then decreased gradually, whereas NMT2 mRNA expression was inversely regulated, showing that NMT1 is the main NMT enzyme early in embryonic development. As recently suggested in human [22], the expression level of NMT2 could therefore be linked to NMT1 level. Therefore, further studies are needed to understand the possible coordinate regulation of NMT1 and NMT2 in the rat, especially throughout embryonic development.

Acknowledgements

The antibody to human myristoyl-CoA: protein N-myristoyltransferase 1 was a generous gift from Dr. B.F. Cravatt (The Scripps Research Institute, La Jolla, CA). We thank M. Brochet, C. Blouin, M. Bouriel, and K.L. Cung for able technical assistance and animal care.

References

1. Johnson DR, Bhatnagar RS, Knoll LJ, Gordon JI: Genetic and biochemical studies of protein *N*-myristoylation. Annu Rev Biochem 63: 869–914, 1994
2. Casey PJ: Protein lipidation in cell signaling. Science 268: 221–225, 1995
3. Resh MD: Myristylation and palmitylation of SRC family members: the fats of the matter. Cell 76: 411–413, 1999
4. Maurer-Stroh S, Eisenhaber F: Myristoylation of viral and bacterial proteins. Trends Microbiol 12: 178–185, 2004
5. Ozols J, Carr SA, Strittmatter P: Identification of the NH_2-terminal blocking group of NADH cytochrome b5 reductase as myristic acid and the complete amino acid sequence of the membrane-binding domain. J Biol Chem 259: 13349–13354, 1984
6. Maurer-Stroh S, Gouda M, Novatchkova M, Schleiffer A, Schneider G, Sirota FL, Wildpaner M, Hayashi N, Eisenhaber F: MYRbase: analysis of genome-wide glycine myristoylation enlarges the functional spectrum of eukaryotic myristoylated proteins. Genome Biology 5: R21 1–16, 2004
7. Boisson B, Giglione C, Meinnel T: Unexpected protein families including cell defense components feature in the N-myristoylome of a higher eukaryote. J Biol Chem 278: 43418–43429, 2003
8. Towler DA, Adams SP, Eubanks SR, Towery DS, Jackson-Machelski E, Glaser L, Gordon JI: Purification and characterization of yeast myristoyl-CoA: protein N-myristoyltransferase. Proc Natl Acad Sci USA 87: 2708–2712, 1987
9. Duronio RJ, Towler DA, Heuckeroth RO, Gordon JI: Disruption of the yeast N-myristoyltransferase gene causes recessive lethality. Science 243: 796–800, 1989
10. Ntwasa M, Egerton M, Gay NJ: Sequence and expression of Drosophila myristoyl-CoA:protein N-myristoyltransferase: evidence for proteolytic processing and membrane localisation. J Cell Sci 110: 149–156, 1997
11. Qi Q, Rajala RVS, Anderson W, Jiang C, Rozwadowski K, Selvaraj G, Sharma R, Datla R: Molecular cloning, genomic organization, and biochemical characterization of myristoyl-CoA:protein N-myristoyltransferase from Arabidopsis thaliana. J Biol Chem 275: 9673–9683, 2000
12. Dumonceaux T, Rajala RV, Sharma R, Selvaraj G, Datla R: Molecular characterization of a gene encoding N-myristoyltransferase (NMT) from Triticum aestivum (bread wheat). Genome 47: 1036–1042, 2004
13. Gunaratne RS, Sajid M, Ling IT, Tripathi R, Pachebat JA, Holder AA: Characterization of N-myristoyltransferase from Plasmodium falciparum. Biochem J 348: 459–463, 2000
14. Price HP, Menon MR, Panethymitaki C, Goulding D, McKean PG, Smith DF: Myristoyl-CoA: protein N-myristoyltransferase, an essential enzyme and potential drug target in kinetoplastid parasites. J Biol Chem 278: 7206–7214, 2003
15. Glover CJ, Goddard C, Felsted RL: N-myristoylation of p60src. Identification of a myristoyl-CoA: glycylpeptide N-myristoyltransferase in rat tissues. Biochem J 250: 485–491, 1988
16. McIlhinney RAJ, Young K, Egerton M, Camble R, White A, Soloviev M: Characterization of human and rat brain myristoyl-CoA:protein N-myristoyltransferase: evidence for an alternative splice variant of the enzyme. Biochem J 333: 491–495, 1998
17. Giang DK, Cravatt BF: A second mammalian N-myristoyltransferase. J Biol Chem 273: 6595–6598, 1998
18. Weston SA, Camble R, Colls J, Rosenbrock G, Taylor I, Egerton M, Tucker AD, Tunnicliffe A, Mistry A, Mancia F, de la Fortelle E, Irwin J, Bricogne G, Pauptit RA: Crystal structure of the anti-fungal target N-myristoyltransferase. Nat Struct Biol 5: 213–221, 1998
19. Bhatnagar RS, Futterer K, Farazi S, Korolev S, Murray CL, Jackson-Machelski E, Gokel GW, Gordon JI, Waksman G: Structure of N-myristoyltransferase with bound myristoylCoA and peptide substrate analogs. Nat Struct Biol 5: 1091–1097, 1998
20. Rundle DR, Rajala RVS, Anderson RE: Characterization of type I and type II myristoyl-CoA: protein N-myristoyltransferase with the acyl-CoAs found on heterogeneously acylated retinal proteins. Exp Eye Res 75: 87–97, 2002
21. Yang SH, Shrivastav A, Kosinski C, Sharma RK, Chen M-H, Berthiaume LG, Peters LL, Chuang P-T, Young SG, Bergo MO: N-myristoyltransferase 1 is essential in early mouse development. J Biol Chem 280: 18990–18995, 2005
22. Ducker CE, Upson JJ, French KJ, Smith CD: Two N-myristoyltransferase isozymes play unique roles in protein myristoylation, proliferation, and apoptosis. Mol. Cancer Res 3: 463–476, 2005
23. Towler DA, Adams SP, Eubanks SR, Towery DS, Jackson-Machelski E, Glaser L, Gordon JI: Myristoyl-CoA: protein N-myristoyltransferase activities from rat liver and yeast possess overlapping yet distinct peptide substrate specificities. J Biol Chem 263: 1784–1790, 1988
24. Rioux V, Galat A, Jan G, Vinci F, D'Andréa S, Legrand P: Exogenous myristic acid acylates proteins in cultured rat hepatocytes. J Nutr Biochem 13: 66–74, 2002
25. Rioux V, Daval S, Guillou H, Jan S, Legrand P: Although it is rapidly metabolized in cultured rat hepatocytes, lauric acid is used for protein acylation. Reprod Nutr Dev 43: 419–430, 2003
26. Towler DA, Glaser L: Protein fatty acid acylation: enzymatic synthesis of an N-myristoylglycyl peptide. Proc Natl Acad Sci USA 83: 812–2816, 1986
27. D'Andrea S, Guillou H, Jan S, Catheline D, Thibault J-N, Bouriel M, Rioux V, Legrand P: The same rat Δ6-desaturase not only acts on 18- but also on 24-carbon fatty acids in very-long-chain polyunsaturated fatty acid biosynthesis. Biochem J 364: 49–55, 2002
28. Bensadoun A, Weinstein D: Assay of proteins in the presence of interfering materials. Anal Biochem 70: 241–250, 1976
29. Borgese N, Aggujaro D, Carrera P, Pietrini G, Bassetti M: A role for N-myristoylation in protein targeting: NADH-cytochrome b5 reductase requires myristic acid for association with outer mitochondrial but not ER membranes. J Cell Biol 135: 1501–1513, 1996
30. Guillou H, D'Andréa S, Rioux V, Barnouin R, Dalaine S, Pedrono F, Jan S, Legrand P: Distinct roles of endoplasmic reticulum cytochrome b5 and fused cytochrome b5-like domain for rat Δ6-desaturase activity. J Lipid Res 45: 32–40, 2004
31. Duronio RJ, Reed SI, Gordon JI: Mutations of human myristoyl-CoA: protein N-myristoyltransferase cause temperature-sensitive myristic auxotrophy in Saccharomyces cerevisiae. Proc Natl Acad Sci USA 89: 4129–4133, 1992
32. Glover CJ, Hartman KD, Felsted RL: Human N-myristoyltransferase amino-terminal domain involved in targeting the enzyme to the ribosomal subcellular fraction. J Biol Chem 272: 28680–28689, 1997
33. Raju RVS, Datla RSS, Sharma RK: Genomic organization of human myristoyl-CoA: protein N-myristoyltransferase. Biochem Biophys Res Commun 257: 284–288, 1999
34. Selvakumar P, Pasha MK, Ashakumary L, Dimmock JR, Sharma RK: Myristoyl-CoA: protein N-myristoyltransferase: a novel molecular approach for cancer therapy. Int J Mol Med 10: 493–500, 2002